Average elastic fields and scale-dependent overall properties of heterogeneous micropolar materials containing spherical and cylindrical inhomogeneities

P. Sharma*
General Electric Corporate Research & Development, Niskayuna, New York, 12309

A. Dasgupta
University of Maryland, College Park, Maryland 20742

(Received 14 May 2002; revised manuscript received 27 August 2002; published 17 December 2002)

Scale-dependent solutions are provided for the ''average'' elastic fields, when spherical and cylindrical inhomogeneities are embedded in an infinite micropolar medium. A mean-field homogenization technique is extended to a micropolar medium and the overall scale-dependent properties of micropolar composite are computed and compared with the classical solution. Unlike classical elastic solutions (which are scale-independent), the apparent stiffness of isotropic micropolar composites increases as inhomogeneity size decreases, at a constant volume fraction. In transversely isotropic micropolar composites, a more complex orientation-dependent behavior is observed: the apparent microscale stiffness for transverse shear and axial extension increase with decreasing inhomogeneity size (as in the isotropic case), while the transverse bulk stiffness exhibits the opposite trend. The current work is expected to find application in the analysis of nanocomposites, biocomposites, and foam structures.

DOI: 10.1103/PhysRevB.66.224110 PACS number(s): 62.20.Dc, 62.25.+g, 83.80.Ab

I. INTRODUCTION

As has been noted by several researchers, e.g., Eringen,[1] and Lakes,[2] classical elasticity becomes inaccurate when the length scales of structural constituents become comparable to the intrinsic characteristic length scale of the material micromorphology, or nanomorphology. Granular media, materials with microstructures, composite materials, biological media (blood, bones, etc.), nanoscale materials, and foams are examples of such structures. The use of the more enriched micropolar theory of elasticity is often warranted in such situations. The theory of micropolar elasticity was firmly established by Eringen and co-workers[1,3–5] in several papers and monographs. In particular, much of the work in this area was recently summarized by Eringen.[1] Several other researchers have contributed to the general field of Cosserat elasticity, and Refs. 6–9 also provided extensive lists of references, as well as overviews of the subject.

In the micromorphic representation of media, materials are idealized at each point to possess individual deformable directors. Deformations of such materials are then constructed by superposing the classical macroscale deformation fields with the local (or microscale) deformations of the deformable directors. In classical continuum mechanics, kinematical degrees of freedom are based on macroscale material point translations that also uniquely define macroscale rotations. Classical continuum media thus do not possess independent rotational degrees of freedom. However, material points in micromorphic media can possess, in addition to the classical macroscale displacement fields, microshear, microelongations, and microrotations (which are distinct from the classical macroscale rotations). Simplified versions of the micromorphic continuum include the microstretch medium (that possesses microelongation and microrotational degrees of freedoms in addition to the classical ones) and the micropolar continuum (whose deformation directors only have rotational degrees of freedom in addition to the classical ones). The micropolar medium is the object of this study and has several similarities to the Cosserat media.[1] The concept of classical, micropolar, microstretch, and micromorphic (3M) media is depicted and discussed in Fig. 1. Clearly, the ''discrete'' media concept embodied in 3M media is ideal for materials at the nanoscale or where additional degrees of freedom are likely to have an impact.

The micropolar medium concept was applied to biological materials, cellular solids, polymers, etc.,[10–12] and future applications are predicted for nanoscale materials and structures. In particular reference to the nanoscale, some recent and interesting research[13,14] indicated that independent microrotations or nanorotations are important deformation mechanisms in nanostructures. As can be well appreciated, the material systems discussed above (i.e., those that can be modeled as micropolar materials, e.g., biocomposites, cellular solids, and nanostructured solids) are often composites or heterogeneous media (or can be treated as such). Their properties are scale dependent, and an estimation of their effective properties is of great technological interest. Such estimates require a knowledge of the ''average'' micropolar elastic fields caused throughout the material heterogeneities, because of external loading.

Extensive work has been done in the field of micromechanics of inclusions and inhomogeneities in classical elastic media. Some excellent reviews have been provided by Mura and co-workers[15–17] and Nemat-Nasser and Hori.[18] In contrast, little attention has been paid to inclusions and inhomogeneities in a Cosserat or micropolar medium. Recently, two papers[19,20] addressed the problems of spherical and cylindrical inclusions, respectively. Mura[17] defined an *inclusion* as a bounded region in a matrix, with a stress-free transformation strain or eigenstrain prescribed in the region. An *inhomogeneity* is defined as a bounded region in a matrix, with different material properties than those of the surrounding matrix.

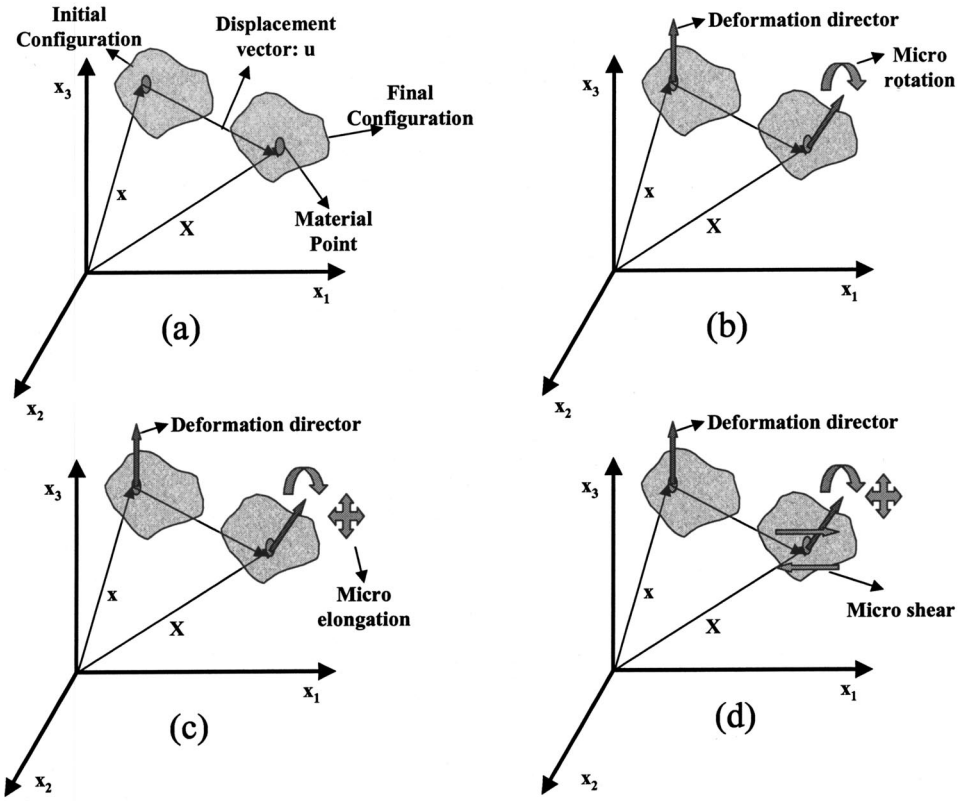

FIG. 1. Schematic of the 3 M concept contrasted with classical continuum (a), classical (b), micropolar (c), one microstretch (d) micromorphics. Here the lower case *x* represents the undeformed configuration while the upper case *x* represents the deformed configuration.

Various examples of naturally occurring eigenstrains are thermal expansion, electromechanical or magnetomechanical strains, plastic deformation, hygromechanical swelling strain, etc. Eshelby[25,26] showed that the elastic field of an inhomogeneity could be obtained by replacing the inhomogeneity with an equivalent inclusion containing a prescribed fictitious eigenstrain of an appropriate magnitude.

To our knowledge, the problem of an *inhomogeneity* in a micropolar material has not been addressed in closed form before. In particular, no closed-form solution for the overall properties of Cosserat materials reinforced by inhomogeneities has appeared in the literature. There is no literature on the use of Eshelby's[25,26] celebrated equivalent inclusion method in scale-dependent homogenization methods for micropolar materials (unlike in classical elasticity, where most homogenization methods are scale-independent and are based on Eshelby's approach). In general, researchers have tended to follow the numerical route as far as applications of Cosserat elasticity to composites is concerned.

The scant work that is available in the literature on homogenization in Cosserat materials is discussed here. Yuan and Tomita[21,22] used finite-element simulations (unit-cell method) to compute the overall properties of Cosserat materials with periodically distributed voids. They presented scale-dependent effective properties. Recently Forest[23] presented some fundamental work on the study of size effects in solids via the use of Cosserat elasticity. The authors of Ref. 24 presented a finite element approach to estimate elastoplastic overall properties of Cosserat materials.

In this paper, we use Eshelby's formalism of eigenstrains,[25,26] modified appropriately to account approximately for interactions between inhomogeneities, to estimate average stresses in spherical and cylindrical inhomogeneities embedded in micropolar materials. Extending a classical mean-field homogenization scheme,[27,28] we obtain overall scale-dependent properties for micropolar composites based on these average elastic fields.

II. MICROPOLAR CONSTITUTIVE LAWS AND ESHELBY'S EQUIVALENT INCLUSION CONCEPT

Let a micropolar inclusion be enclosed in an infinite micropolar medium with prescribed asymmetric stress-free eigenstrain, and eigentorsion. Both the eigenstrain (ε_{ij}^{*}) and eigentorsion (κ_{ij}^{*}) are considered to be zero outside the domain of the inclusion (Ω) and uniform within it. The governing equations for the micropolar medium within the domain of the inclusion can be written as[1,19]

$$\sigma_{ij,j}=0, \tag{1a}$$

$$m_{ji,j}+\eta_{ijk}\sigma_{jk}=0, \tag{1b}$$

$$\sigma_{ji}=C_{ijkl}(\varepsilon_{kl}-\varepsilon_{kl}^{*}), \tag{2a}$$

$$m_{ji}=D_{ijkl}(\kappa_{kl}-\kappa_{kl}^{*}), \tag{2b}$$

$$\varepsilon_{ji}=u_{i,j}-\eta_{jik}\varphi_{k}, \tag{3a}$$

$$\kappa_{ji}=\varphi_{i,j}. \tag{3b}$$

Typical summation rules apply (unless otherwise noted). σ is the regular stress tensor, while m denotes the moment stress tensor. C and D are the fourth-order elasticity tensors. In this paper we assume micropolar centrosymmetric isotropic be-

havior for all materials. u and φ are the displacement and microrotation vectors, respectively, and ε and κ are the strain and torsion tensors, respectively. η_{ijk} is the alternating tensor. The elastic properties for an isotropic centrosymmetric micropolar material can be written as.

$$C_{jikl}=\lambda\,\delta_{ji}\delta_{kl}+\left(\mu+\frac{\kappa}{2}\right)\delta_{jk}\delta_{il}+\left(\mu-\frac{\kappa}{2}\right)\delta_{ik}\delta_{jl}, \quad (4a)$$

$$D_{jikl}=\alpha\,\delta_{ji}\delta_{kl}+\gamma\,\delta_{jk}\delta_{il}+\beta\,\delta_{ik}\delta_{jl}, \quad (4b)$$

where α, β, λ, γ, κ, and μ are the six micropolar elastic constants required to completely specify the fourth order micropolar material property tensors.

In this work, we assume that the inhomogeneity is perfectly bonded to the matrix. Most work in classical elastic theory of composites adopt such an assumption (see for example, Mura[17]). However, in certain cases such an assumption ceases to be valid and several researchers have developed theories for inhomogeneities that are imperfectly bonded to the matrix (within the context of classical elasticity).[29–31] Analogous theories are not available in the micropolar theory of inhomogeneities, and are beyond the scope of the present paper.

According to Eshelby's formalism, the stress disturbance due to an elastic inhomogeneity embedded in an infinite elastic matrix (subjected to uniform far field strain ε^0) can be found by using the ''equivalent inclusion'' concept. Accordingly, an inhomogeneity can be replaced by an inclusion with a suitable fictitious eigenstrain prescribed within its domain. Let the inhomogeneity have a pre-existing inelastic strain (eigenstrain) ε^p. Then, this inhomogeneity can be replaced by an equivalent inclusion with a suitable fictitious eigenstrain ε^*.

This fictitious eigenstrain is determined by equating the stress in the inhomogeneity to the stress everywhere within the equivalent inclusion (V_Ω):

$$\begin{aligned}\sigma_{ij}&=C_{ijkl}(\varepsilon^o_{kl}+S_{klmn}(\varepsilon^*_{mn}+\varepsilon^p_{mn})-\varepsilon^*_{kl}-\varepsilon^p_{kl})\\&=C^h_{ijkl}[\varepsilon^o_{kl}+S_{klmn}(\varepsilon^*_{mn}+\varepsilon^p_{mn})-\varepsilon^p_{kl}].\end{aligned} \quad (5)$$

Here S is the so-called Eshelby tensor for interior points (i.e., for all position vectors lying completely within the inhomogeneity). C is the fourth-order elastic stiffness tensor for the matrix material, while C^h is the elastic tensor for the inhomogeneity. For an inhomogeneity of arbitrary shape, S is an integral operator on $(\varepsilon^*+\varepsilon^p)$. In such a case, Eq. (5) are a set of six simultaneous integral equations that must be solved within the region of the inhomogeneity to determine the fictitious (and generally nonuniform eigenstrain). In a classical elastic medium, Eshelby's tensor is uniform for ellipsoidal shapes (which includes spheres and cylinders). In such a case, Eq. (5) reduce to six algebraic equations, and the problem of an ellipsoidal inhomogeneity can thus be readily solved. Unfortunately, Eshelby's tensor is nonuniform for the micropolar case for all geometries,[19,20,32] and the nonuniform fictitious eigenstrain can be found only numerically. It should be noted that the integral operator S has a very simple physical meaning: for a given total eigenstrain (fictitious or otherwise), this operator relates the actual strain perturbation to the eigenstrain, i.e., the perturbation strain is S: $(\varepsilon^*+\varepsilon^p)$. In the left-hand side of Eqs. (5), where the stress within the inhomogeneity is expressed in terms of the matrix moduli, both the fictitious and the real eigenstrains are subtracted since these are inelastic strains and do not participate in the elastic constitutive behavior. On the other hand, on the right-hand side, where the stresses are expressed in terms of the inhomogeneity moduli, only the real eigenstrain (ε^p) is subtracted. The use of Eshelby's equivalent inclusion principle for the micropolar case is discussed in Sec. III, where we make a suitable approximation to facilitate the estimation of the average scale-dependent stresses and overall properties.

III. SOLUTION

In this paper, we are interested only in the average stresses in the matrix and inhomogeneity, and the overall effective properties that are scale dependent. In such a case, we propose to simplify the analysis by using volumetrically averaged micropolar equivalents of Eshelby's tensors. This assumption cannot be employed to estimate local pointwise stress distributions, but often provides reasonable estimates of the average stresses in the inhomogeneity/matrix for the purpose of estimating overall properties.[33] Furthermore, as will be shown, the averaging process does not eliminate the scale dependence. This averaging process leads to the estimation of an ''average'' or ''smeared'' fictitious eigenstrain and eigentorsion, which can then be used to compute the average stresses as well as the overall homogenized properties of a micropolar composite. Further discussion of this simplification and its implications are presented in Sec. IV. In this section, the average micropolar Eshelby-type tensors are derived for spherical inhomogeneities and the Mori-Tanaka mean-field homogenization scheme for classical elasticity[27,28] is extended to micropolar materials. We also present parametric examples of scale-dependent overall properties of micropolar composites reinforced by cylindrical inhomogeneities.

Cheng and He[19,20] and Sharma and Dasgupta[32] used the Green functions of micropolar elasticity to obtain Eshelby's nonuniform tensors for spherical inclusions, circular-cylindrical inclusions, and cuboidal inclusions, respectively. In micropolar materials, four Eshelby-type tensors are needed to relate the eigenstrains and eigentorsions to the perturbations in strains and torsions, as shown in Eqs. (6a) and (6b),

$$\varepsilon_{mn}=K_{mnji}\varepsilon^*_{ji}+L_{mnji}\kappa^*_{ji}, \quad (6a)$$

$$\kappa_{mn}=\hat{K}_{mnji}\varepsilon^*_{ji}+\hat{L}_{mnji}\kappa^*_{ji}, \quad (6b)$$

where K, $\hat{K}$, L, and $\hat{L}$ are the micropolar Eshelby tensors, expressed as[19]

$$K_{mnji}=I^S_{nji,m}+I_{nji,m}-\varepsilon_{lmn}\hat{I}_{lji}, \quad (7a)$$

$$L_{mnji}=J_{nji,m}-\varepsilon_{lmn}\hat{J}_{lji}, \quad (7b)$$

$$\hat{K}_{mnji} = \hat{I}_{nji,m}, \tag{7c}$$

$$\hat{L}_{mnji} = \hat{J}_{nji,m}. \tag{7d}$$

Here we have followed the notation of Cheng and He.[19,20] More information about these tensors is summarized in Appendix A for completeness [Eqs. (A1a)–(A1e)]. Note that Eqs. (6a) and (6b), similar to Eshelby's integral operator S, relate the perturbed strain and perturbed torsion to the eigenstrain and the eigentorsion, respectively, in terms of operators K, $\hat{K}$, L, and $\hat{L}$. The actual strains and torsions are coupled to each other due to the L and $\hat{L}$ operators.

Ignoring the presence of any real eigenstrains (ε^p), which are of no consequence in the calculation of overall properties, the micropolar version of Eshelby's equivalent inclusion conditions [Eqs. (5)] can be written as

$$\begin{aligned}\sigma_{ij} &= C_{ijkl}(\varepsilon^o_{kl} + K_{klmn}\varepsilon^*_{mn} + L_{klmn}\kappa^*_{mn} - \varepsilon^*_{kl}) \\ &= C^h_{ijkl}(\varepsilon^o_{kl} + K_{klmn}\varepsilon^*_{mn} + L_{klmn}\kappa^*_{mn}),\end{aligned} \tag{8a}$$

$$\begin{aligned}m_{ij} &= D_{ijkl}(\kappa^o_{kl} + \hat{K}_{klmn}\varepsilon^*_{mn} + \hat{L}_{klmn}\kappa^*_{mn} - \kappa^*_{kl}) \\ &= D^h_{ijkl}(\kappa^o_{kl} + \hat{K}_{klmn}\varepsilon^*_{mn} + \hat{L}_{klmn}\kappa^*_{mn}).\end{aligned} \tag{8b}$$

As can be seen from Eqs. (A1a)–(A1e) in Appendix A, the four micropolar Eshelby tensors are expressed in terms of the tensors $\hat{I}$, I, J, and $\hat{J}$. These, in turn, can be expressed in terms of derivatives of certain potentials, which are expressed mathematically as

$$\psi(\mathbf{x}) = \frac{1}{4\pi}\int\int\int_{\Omega} r\,d\mathbf{x}', \tag{9a}$$

$$\phi(\mathbf{x}) = \frac{1}{4\pi}\int\int\int_{\Omega} \frac{1}{r}\,d\mathbf{x}', \tag{9b}$$

$$M(\mathbf{x},k) = \frac{1}{4\pi}\int\int\int_{\Omega} \frac{e^{-r/k}}{r}\,d\mathbf{x}'. \tag{9c}$$

Here, Ω is the domain of the inhomogeneity, which in our case is either a sphere or a circular cylinder. The origin of the coordinate system is taken to be at the centroid of the inclusion (for both the sphere and the cylinder). The first two potentials are the biharmonic and harmonic potentials while the third is what the authors have termed an exponentially-decaying-density potential (EDD potential).[32] The symbol r is the scalar distance between the spatial coordinates of the integration point and the physical location where the potential is sought to be evaluated. The symbol k is a constant whose value depends on the micropolar material properties (see Appendix A).

The derivatives of the harmonic and biharmonic potentials can be obtained from Mura.[15] The derivatives of $M(x_i,k)$ are described in Appendix B for the spherical case, and in Appendix D for the cylindrical case. The derivatives of the EDD potential are nonuniform within the region of the inclusion shape (sphere or cylinder) and thus, as remarked earlier, the micropolar Eshelby tensors are non-uniform, even in the case of spheres (unlike in classical elasticity). This fact makes Eqs. (8a) and (8b), in general, analytically intractable. One has to resort to numerical techniques to compute the fictitious non-uniform eigenstrain and eigentorsion. However, since we are interested in analytical estimates of the overall effective properties, we will use the volumetric averages of the micropolar Eshelby tensors, to estimate the average fields in the inhomogeneity problem. Thus Eqs. (8a) and (8b) are replaced by

$$\begin{aligned}\sigma_{ij} &\cong C_{ijkl}(\varepsilon^o_{kl}\langle K_{klmn}\rangle\varepsilon^*_{mn} + \langle L_{klmn}\rangle\kappa^*_{mn} - \varepsilon^*_{kl}) \\ &\cong C^h_{ijkl}(\varepsilon^o_{kl} + \langle K_{klmn}\rangle\varepsilon^*_{mn} + \langle L_{klmn}\rangle\kappa^*_{mn}),\end{aligned} \tag{10a}$$

$$\begin{aligned}m_{ij} &\cong D_{ijkl}(\kappa^o_{kl} + \langle \hat{K}_{klmn}\rangle\varepsilon^*_{mn} + \langle \hat{L}_{klmn}\rangle\kappa^*_{mn} - \kappa^*_{kl}) \\ &\cong D^h_{ijkl}(\kappa^o_{kl} + \langle \hat{K}_{klmn}\rangle\varepsilon^*_{mn} + \langle \hat{L}_{klmn}\rangle\kappa^*_{mn}).\end{aligned} \tag{10b}$$

The angular brackets indicate averaging over the volume of the inhomogeneity. The average of any tensor field is defined as

$$\langle F_{ijk\ldots}(\mathbf{x})\rangle = \frac{1}{V_\Omega}\int\int\int_{\Omega} F_{ijk\ldots}(\mathbf{x})\,dV. \tag{11}$$

Here F is any arbitrary order tensor field, while V_Ω is the volume of the region of the inhomogeneity Ω.

The volumetrically averaged Eshelby tensors for a spherical inclusion in a micropolar material are not available in the literature, and are derived by the present authors in this section. For the circular-cylindrical inclusion, we can easily obtain the average Eshelby micropolar tensors since the averages of the EDD potential and their derivatives were presented by Cheng and He[20] in their calculation of the strain energy for a circular-cylindrical inclusion (summarized in Appendix D of this paper).

Consider the spherical shape. The expressions of the derivatives of ϕ (harmonic potential), ψ (biharmonic potential), and $M(x_i,k)$ (EDD potential) are presented in Appendix B. The volumetric averages of these quantities are derived in detail in Appendix C. The main results are expressed here as

$$\langle \phi_{,ij}\rangle = \frac{-1}{3}(\delta_{mi}\delta_{mj}), \tag{12a}$$

$$\begin{aligned}\langle \psi_{,ijkl}\rangle = \frac{-1}{15}[&(\delta_{mk}\delta_{mj})(\delta_{nl}\delta_{ni}) + (\delta_{ml}\delta_{mj})(\delta_{nk}\delta_{ni}) \\ &+ 2(\delta_{mk}\delta_{ml})(gd_{nj}\delta_{ni})],\end{aligned} \tag{12b}$$

$$\langle M(k)\rangle = k^2 + \frac{k\Phi(k)}{V}P_1, \tag{12c}$$

$$\langle M_{,i}(k)\rangle = 0, \tag{12d}$$

$$\langle M_{,ij}(k)\rangle = \frac{\delta_{ij}\Phi(k)}{ikV}P_2 - \frac{\delta_{ij}\Phi(k)}{k^2V}P_{3ij}, \tag{12e}$$

$$\langle M_{,ijk}(k)\rangle = 0, \tag{12f}$$

$$\begin{aligned}\langle M_{,ijkl}(k)\rangle = &-\frac{\Phi(k)}{k^2V}(\delta_{ij}\delta_{kl}+\delta_{ik}\delta_{jl}+\delta_{il}\delta_{jk})P_4 \\ &-\frac{\Phi(k)}{ik^3V}(\delta_{kl}P_{5ij}+\delta_{jl}P_{5ik}+\delta_{jk}P_{5il}+\delta_{il}P_{5jk} \\ &+\delta_{ik}P_{5jl}+\delta_{ij}P_{5kl})+\frac{\Phi(k)}{k^4V}P_{6ijkl}.\end{aligned} \tag{12g}$$

Here P_1, P_2, P_{3ij}, P_4, P_{5ij}, and P_{6ijkl} are volume integrals evaluated in the domain of the spherical inhomogeneity and appear in the evaluation of the volumetric averages. They are uniform, but scale-dependent. They are defined and evaluated in Appendix C. Here V is the volume of the spherical inclusion and $\Phi(k)$ is $-k(k+a)e^{-a/k}$. The symbol a represents either the radius of the sphere or the cylinder. Note that the volumetric averages of the odd-order derivatives of the EDD potential vanish over a sphere.

The derivation of the average micropolar Eshelby tensors paves the way for evaluating the average stresses as well as the overall properties. Now we use the combination of Eshelby's equivalent inclusion principle [as defined in Eqs. (10a) and (10b)] and an extended version of a classical mean-field homogenization concept to evaluate the scale-dependent overall properties. The extended mean-field concept for micropolar materials (based on the classical concept) is briefly outlined here.

It is important to note here that for effective properties we need only consider either a uniform couple stress *or* a uniform force stress separately as the far-field boundary condition. Application of both boundary conditions simultaneously will violate equilibrium (or will require nonuniform body moments, needlessly complicating the problem). Let either a self-equilibrating far-field stress field *or* a self-equilibrating moment stress field be applied to a micropolar material containing a finite concentration of similarly oriented but randomly distributed inhomogeneities. Then we have

$$\begin{aligned}\sigma^{\infty}_{ij}+\sigma^{\Omega}_{ij} &= C^{h}_{ijkl}\{(C^{M}_{ijkl})^{-1}(\sigma^{\infty}_{kl}+\sigma^{M}_{kl})+\varepsilon_{kl}) \\ &= C^{M}_{ijkl}\{(C^{M}_{ijkl})^{-1}(\sigma^{\infty}_{kl}+\sigma^{M}_{kl})+\varepsilon_{kl}-\varepsilon^{*}_{kl}),\end{aligned} \tag{13a}$$

$$\begin{aligned}m^{\infty}_{ij}+m^{\Omega}_{ij} &= D^{h}_{ijkl}\{(D^{M}_{ijkl})^{-1}(m^{\infty}_{kl}+m^{M}_{kl})+\kappa_{kl}) \\ &= D^{M}_{ijkl}\{(D^{M}_{ijkl})^{-1}(m^{\infty}_{kl}+m^{M}_{kl})+\kappa_{kl}-\kappa^{*}_{kl}).\end{aligned} \tag{13b}$$

Here σ^{Ω} and σ^{M} are the average stress disturbances in the inhomogeneity and in the matrix, respectively, due to the presence of the inhomogeneities; while m^{Ω} and m^{M} are the analogous tensors for the moment-stress. The superscript ∞ indicates far-field values, and ε^{*} and κ^{*} are the fictitious eigenstrain and eigentorsion, respectively, necessary to replace the inhomogeneity by an inclusion of the same geometry. Finally, ε is the strain perturbation due to the presence of a single inhomogeneity and κ is the analogous torsion perturbation. In subsequent derivations, although both moment-stress and force-stress equations are included together, when evaluating effective properties, they are applied at the far-field individually (not simultaneously) and the fictitious eigenfield related to the other should be considered to be zero. In our numerical examples of computing effective stiffness of micropolar composites (to be presented in Sec. IV), a uniform far-field force stress boundary conditions will be considered while the far-field moment stress boundary condition will be set to zero. Such a set of boundary conditions implies that $\sigma^{\infty}_{ji}=\sigma^{\infty}_{ij}$. Decomposing the isotropic centrosymmetric micropolar constitutive relation into its symmetric and antisymmetric parts, it can be shown that the constitutive relation for the force stress should be written as $\sigma_{ji}=C_{(ji)(kl)}\varepsilon_{(kl)}$. Here the parentheses indicate the symmetric part of the tensors with respect to those indices. In the sequel, this condition will not be explicitly written, although it should be understood by the reader to apply throughout the remaining equations.

Using, the average micropolar Eshelby tensors derived in this section, we can write

$$\varepsilon_{mn}=\langle K_{mnji}\rangle\varepsilon^{*}_{ji}+\langle L_{mnji}\rangle\kappa^{*}_{ji}, \tag{14a}$$

$$\kappa_{mn}=\langle \hat{K}_{mnji}\rangle\varepsilon^{*}_{ji}+\langle \hat{L}_{mnji}\rangle\kappa^{*}_{ji}. \tag{14b}$$

Now, as per the mean-field concept, the average of all the stress disturbances must be zero, i.e.,

$$(1-f)\sigma^{M}_{ij}+f\sigma^{\Omega}_{ij}=0, \tag{15a}$$

$$(1-f)m^{M}_{ij}+fm^{\Omega}_{ij}=0. \tag{15b}$$

Here f is the volume fraction of the inhomogeneities. Using Equations (13a), (13b), (14a), (14b), (15a) and (15b), the following can be derived easily:

$$\sigma^{M}_{ij}=-fC^{M}_{ijkl}[(\langle K_{klmn}\rangle_{klmn}-\delta_{klmn})\varepsilon^{*}_{mn}+\langle L_{klmn}\rangle\kappa^{*}_{mn}], \tag{16a}$$

$$m^{M}_{ij}=-fD^{M}_{ijkl}[\langle \hat{K}_{klmn}\rangle_{klmn}\varepsilon^{*}_{mn}+\langle \hat{L}_{klmn}-\delta_{klmn}\rangle\kappa^{*}_{mn}], \tag{16b}$$

$$\sigma^{\Omega}_{ij}=(1-f)C^{M}_{ijkl}[(\langle K_{klmn}\rangle_{klmn}-\delta_{klmn})\varepsilon^{*}_{mn}+\langle L_{klmn}\rangle\kappa^{*}_{mn}], \tag{16c}$$

$$m^{\Omega}_{ij}=(1-f)D^{M}_{ijkl}[\langle \hat{K}_{klmn}\rangle_{klmn}\varepsilon^{*}_{mn}+\langle \hat{L}_{klmn}-\delta_{klmn}\rangle\kappa^{*}_{mn}]. \tag{16d}$$

Here δ_{ijkl} is the fourth-order Kronecker tensor.

Finally, approximate average values of the fictitious eigenstrains and eigentorsions can be computed by substituting Eqs. (16a)–(16d) and Eqs. (13a) and (13b). The final expressions are given below:

$$\begin{aligned}&[\Delta C_{ijkl}\{f(\langle K_{klmn}\rangle-\delta_{klmn})-\langle K_{klmn}\rangle\}+C^{M}klmn]\varepsilon^{*}_{mn} \\ &\quad-\Delta C_{ijkl}\langle L_{klmn}\rangle\kappa^{*}_{mn}=\Delta C_{ijkl}\varepsilon^{\infty}_{kl},\end{aligned} \tag{17a}$$

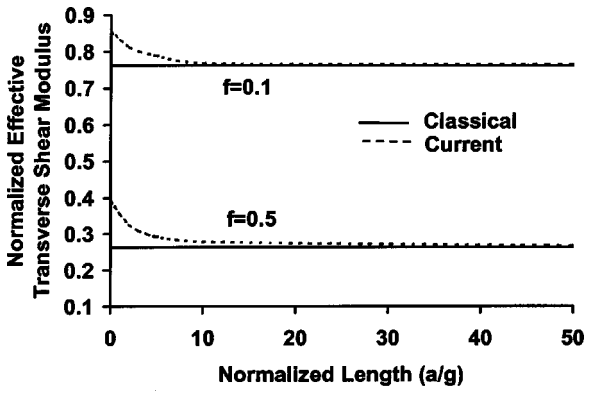

FIG. 2. Effective normalized transverse shear modulus for randomly dispersed circular cylindrical voids vs the normalized length for the varying volume fraction (f) at a fixed micropolarity ($p=0.5$). Here the symbol a is the radius of the cylindrical voids, while g is the normalizing parameter (see Appendix A).

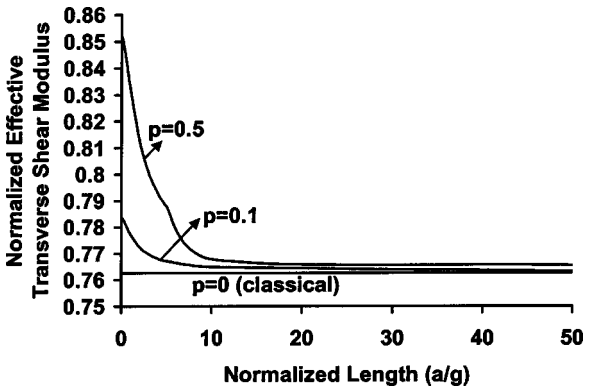

FIG. 3. Effective normalized transverse shear modulus for randomly dispersed circular cylindrical voids vs the normalized length for the varying micropolarity (p) at a fixed volume fraction ($f=0.5$). Here the symbol a is the radius of the cylindrical voids, while g is the normalizing parameter (see Appendix A).

$$-\Delta D_{ijkl}\langle \hat{L}_{klmn}\rangle \varepsilon^{*}_{mn}+[\Delta D_{ijkl}\{f(\langle \hat{K}_{klmn}\rangle-\delta_{klmn}) -\langle \hat{K}_{klmn}\rangle\}+C^{M}klmn]\kappa^{*}_{mn}=\Delta C_{ijkl}\kappa^{\infty}_{kl}. \quad (17b)$$

Equations (17) represent twelve equations to solve for twelve independent components of eigenstrain and eigentorsion. The overall scale-dependent properties $\overline{\mathbf{C}}$ can now be evaluated easily as

$$\overline{\varepsilon}=\mathbf{f}(\varepsilon^{\infty}+\varepsilon^{\Omega})+(1+f)(\varepsilon^{\infty}+\varepsilon^{M})=\overline{C}^{-1}\sigma^{\infty}, \quad (18a)$$

$$\varepsilon^{\Omega}=C^{-1}\sigma^{M}+\varepsilon, \quad (18b)$$

$$\varepsilon^{M}=C^{-1}\sigma^{M}, \quad (18c)$$

where we have used bold-faced notation.

IV. RESULTS AND DISCUSSION

Results are presented for a micropolar matrix with randomly distributed voids (spherical and cylindrical). The cylindrical voids are identically oriented, thus making the voided material transversely isotropic in the apparent macroscale behavior. We consider only uniform far-field force stresses (no moment-stresses), and seek to find the overall properties of the resulting porous composite. Poisson's ratio is fixed at 0.3. The degree of micropolarity, p, is introduced in this article as $p=\kappa/2\mu$.

The transversely isotropic results for the cylindrical case are presented first. Figure 2 depicts the variation of the effective transverse shear modulus (in the 1-2 plane, transverse to the axis of the cylindrical voids) with respect to normalized length scale, for different void volume fractions at a fixed degree of micropolarity ($p=0$ corresponds to the classical elasticity case). The overall effective transverse shear modulus is normalized with that of the matrix and the results are plotted with respect to the normalized length parameter (a/g). Here g is the characteristic length parameter described in Appendix A while a is the radius of the sphere or the circular cylinder. The micropolar shear modulus is calculated as $(C_{1212}+C_{1221})/2$. Our analytical results are consistent with the numerical results presented by Yuan and Tomita.[21,22] It is interesting to note that the micropolar length-scale effect results in the stiffening of the composite (compared with classical predictions) as the void radius decreases. As expected, as the inhomogeneity size (radius) increases, the micropolar solution converges to the classical solution. To explore the effect of degree of micropolarity, the effective transverse shear modulus is presented at a fixed volume fraction of pores, for varying values of p (Fig. 3). Clearly, the degree of micropolarity influences how erroneous the classical predictions might be.

In Fig. 4, we explore the transverse bulk modulus (K_{12}) and the axial extensional modulus (E_{33}) for the case of cylindrical voids. They can be defined as: $K_{12}=(C_{1111}+C_{1122})/2$ and $E_{33}=C_{1111}-2(C_{3322})^2/(C_{2222}+C_{2211})$. Interestingly, as can be seen from Fig. 4, while the effective axial extensional modulus exhibits the same trend as the effective transverse shear modulus (Figs. 2 and 3), the transverse bulk modulus actually *decreases* with a decrease in the

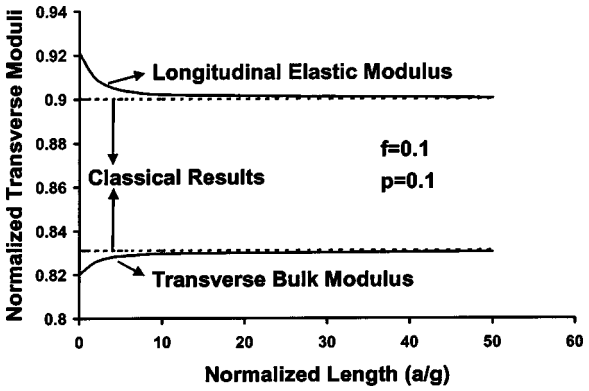

FIG. 4. Effective normalized axial extensional elastic modulus and transverse bulk modulus for randomly dispersed circular cylindrical voids vs the normalized length for fixed micropolarity ($p=0.1$) at a fixed volume fraction ($f=0.1$). Here the symbol a is the radius of the cylindrical voids, while g is the normalizing parameter (see Appendix A).

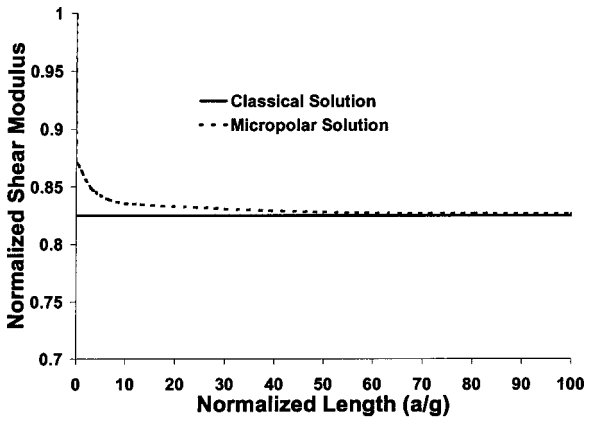

FIG. 5. Effective normalized shear modulus for randomly dispersed spherical voids. The micropolarity (p) is fixed at 0.5 while the volume fraction (f) of the spherical cavities is fixed at 0.1. The symbol a is the spherical void radius and g is the normalizing parameter defined in Appendix A.

void radius. While the trend in effective shear modulus has been reported previously,[21,22] the authors believe that results for the decrease in the transverse bulk modulus are reported here for the first time. These results point out, in addition to the customary length scale effect, a more complex *orientation*-dependent length scale effect. The other transverse property is the axial shear stiffness which we found to follow the same trend as the transverse shear modulus (and hence is not plotted).

Discussion of a subtle point is in order here. As is clear from Eqs. (4a) and (4b) the micropolar constitutive elastic behavior is characterized by two tensors C (which includes classical constants and a micropolar constant κ) and D (which contains micropolar constants, α, β, and γ). Qualitatively, the effect of micropolarity on tensor D is the same as on tensor C, however, in reality (experimentally) one can only measure the ''apparent'' classical shear or bulk modulus for a given solid and indeed these are physically the most intuitive quantities. The micropolar stiffness we plot in Figs. 2–5 represents the modulus that will be determined by a conventional elastic experiment with the micropolar effect entering mainly through the constant κ. For evaluating the effective constants α, β, and γ, moment stress boundary conditions need to be applied instead of force stresses. The effective properties can then be evaluated via Eq. (17b). However, little additional understanding is obtained from such an exercise since experimentally, the determination of α, β, and γ is extremely difficult while the determination of effective $\mathbf{C}$-tensor values (which include the effect of κ) is straightforward. Hence, only C-tensor results are plotted in this work.

The effective isotropic stiffness properties of a micropolar material containing spherical voids is shown in Fig. 5. In this case, due to the symmetry of the inhomogeneity, the effective properties are isotropic and only an increase in the properties with a decrease in the inhomogeneity size is observed.

As emphasized earlier, when evaluating the apparent effective shear modulus of an isotropic micropolar solid (transverse shear for a material containing cylindrical voids), a stiffening is observed (compared to the classical solution) when the inhomogeneity size is decreased below a certain characteristic length. This is the so-called scale effect. This effect is absent in classical elasticity as no length scale enters the constitutive behavior. Indeed, virtually all the homogenization concepts in classical elasticity rely exclusively on scale-independent parameters (e.g., volume fraction) to assess the overall properties. Physically, the length scale effect in micropolar solids arises due to the micro-rotations (i.e. the entrance of strain gradients into the constitutive behavior). The stiffening effect (or softening effect in the case of transverse bulk modulus) observed also has a simple interpretation. Loading of a composite can be considered to be equivalent to supplying energy to the composite. Within the classical framework, almost all the applied energy is dedicated to the classical deformations (i.e. translation of the material points). In the case of a micropolar solid, depending on orientation complexity two scenarios can occur: (i) only part of the energy is spent on classical deformation while a part is expended on micro-rotations. Thus the apparent classical deformations (which are measurable in laboratory) will appear smaller and hence the composite will appear stiffer. (ii) For certain deformation types (i.e., equal biaxial deformation in the plane of transverse isotropy), the additional microscale degrees of rotation facilitate deformation and thus the composite appears softer for that particular deformation mode. One should note that this orientation-dependent softening effect is not observed in an overall isotropic micropolar composite.

It is also pertinent here to discuss the validity of our assumption regarding the use of averaged Eshelby tensors. In the case when local inhomogeneous stresses within and in the vicinity of the inhomogeneity are required, our approximation of first averaging the Eshelby tensors over volume becomes inaccurate. However, we are mainly interested in the overall effective properties and in such a situation our approach is somewhat justified. Perfectly bonded ellipsoidal inclusions are characterized by uniform Eshelby's tensor within the framework of classical elasticity. Nonuniformity of this tensor can arise due to several reasons. For example, the inclusion shape can give rise to nonuniformity. Eshelby's tensor is nonuniform for polyhedrals, even in classical elasticity. Sliding inclusions in general have nonuniform Eshelby tensors. Finally, as in our study inclusions in micropolar material (even ellipsoidal ones) have nonuniform Eshelby tensors.

Our simplifying assumption can be stated as follows. Given an inclusion problem such that Eshelby's tensor is spatially nonuniform, we assume that

$$\langle S_{ijkl}\varepsilon^{*}_{kl}\rangle \cong \langle S_{ijkl}\rangle\langle\varepsilon^{*}_{kl}\rangle. \tag{19}$$

In terms of integral equations, we can recast these equations as follows:[34]

$$S_{ijkl}(x) = \int_V G_{ijkl}(x,y)\,dy, \tag{20a}$$

$$\langle \varepsilon_{ij} \rangle = \frac{1}{V} \int_V \int_V G_{ijkl}(x,y) \varepsilon^*_{kl}(y) dx\, dy$$

$$= \frac{1}{V} \int_V S_{ijkl}(x) \varepsilon^*_{kl}(y) dx = \langle S_{ijkl} \varepsilon^*_{kl} \rangle = \langle S_{ijkl} \rangle \langle \varepsilon^*_{kl} \rangle. \tag{20b}$$

Several researchers have used this approximation.[29,33,35] Nozaki and Taya[35] used this approximation (and the mean-field concept) to compute effective properties of a composite reinforced by convex polygons. Since Eshelby's tensor is not uniform for polyhedrals or polygonals, Rodin[34] questioned the accuracy of Nozaki and Taya's analysis (and by extension, of several previous works dealing with inclusion problems characterized by a nonuniform Eshelby tensor). In a recent paper Nozaki and Taya[33] used the boundary element method to demonstrate that despite the fact that certain shapes (rectangular, pentagonal, etc.) have highly nonuniform stress fields (like in our case for micropolar materials), the assumption in Eq. (27) provides a fair approximation for overall properties. A similar verification of the accuracy of this approximation for our problem (ellipsoidal inhomogeneities in micropolar materials) would require the development of micropolar computational tools (e.g. micropolar finite element or boundary element method), which is beyond the scope of the present paper.

V. SUMMARY

In this paper, Eshelby's equivalent inclusion method was employed to approximately estimate the average micropolar elastic fields of spherical and cylindrical inhomogeneities. For this purpose, the average micropolar Eshelby tensors were derived explicitly. A classical mean-field homogenization scheme was extended to micropolar materials and used in conjunction with the ''averaged'' stresses in the inhomogeneity, to obtain overall scale-dependent stiffness of micropolar composites containing cylindrical and spherical inhomogeneities. Numerical results for selected stiffness components were presented for micropolar materials with voids, by applying appropriate uniform far-field force stresses. The present closed-form solution for randomly distributed voids agrees qualitatively well (for similar volume fractions) with the numerical finite element results presented by Yuan and Tomita[21,22] for micropolar materials containing periodically spaced cylindrical voids. Isotropic materials are found to stiffen as the length scale decreased. As an example, the apparent shear modulus is parametrically explored. In transversely isotropic materials, the size effect on overall properties may have an orientation dependence and may cause stiffening for some stiffness components, but softening for some others. All effective properties are found to monotonically approach the classical elasticity solution as the normalized radius increases, or as the degree of micropolarity decreases.

ACKNOWLEDGMENTS

Financial support and encouragement is acknowledged from General Electric Global Research Center, Nanotechnology AT Program (Dr. Margaret Blohm), and Dr. James Loman.

APPENDIX A: EXPRESSIONS FOR TENSORS $\hat{I}$, I, J, AND $\hat{J}$ IN EQ. (7) (REF. 20)

$$I_{nji} = 2B\mu g^2 \phi_{,ijn} + \frac{\kappa}{\mu}(\delta_{jn}\phi_{,i} - \delta_{in}\phi_{,j}) - 2B\mu g^2 M_{,ijn}(\mathbf{x},g) + \left\{ B\left(\mu + \frac{\kappa}{2}\right) + \frac{\kappa}{2\mu} \right\} \delta_{in} M_{,j}(\mathbf{x},g) + \left\{ B\left(\mu - \frac{\kappa}{2}\right) - \frac{\kappa}{2\mu} \right\} \delta_{jn} M_{,i}(\mathbf{x},g), \tag{A1a}$$

$$J_{nji} = -\frac{1}{2\mu}\{\gamma \varepsilon_{nik}\phi_{,jk} + \beta \varepsilon_{njk}\phi_{,ik}\} + \frac{1}{2\mu}\{\gamma \varepsilon_{nik} M_{,jk}(\mathbf{x},g) + \beta \varepsilon_{njk} M_{,ik}(\mathbf{x},g)\}, \tag{A1b}$$

$$\hat{I}_{nji} = \frac{1}{4\mu}\{\kappa \varepsilon_{ijk}\phi_{,kn} - (2\mu+\kappa)\varepsilon_{nik}\phi_{,jk} - (2\mu-\kappa)\varepsilon_{njk}\phi_{,ik}\} - \frac{1}{4\mu}\{(2\mu+\kappa)\varepsilon_{ijk} M_{,kn}(\mathbf{x},g) - (2\mu+\kappa)\varepsilon_{nik} M_{,jk}(\mathbf{x},g) - (2\mu-\kappa)\varepsilon_{njk} M_{,ik}(\mathbf{x},g)\} + \frac{\varepsilon_{ijk}}{2} M_{,kn}(\mathbf{x},h) + \frac{(2\mu+\kappa)\varepsilon_{ijn}}{4\mu g^2} M(\mathbf{x},g), \tag{A1c}$$

$$\hat{J}_{nji} = -\frac{\gamma+\beta}{4\mu}\phi_{,ijn} + \frac{(2\mu+\kappa)(\gamma+\beta)}{4\mu\kappa} M_{,ijn}(\mathbf{x},g) - \frac{1}{2\kappa}\{\alpha \delta_{ij} M_{,kkn}(\mathbf{x},h) + (\gamma+\beta)\delta_{ij} M_{,ijn}(\mathbf{x},h)\} - \frac{(2\mu+\kappa)}{4\mu\kappa g^2}\{\gamma \delta_{in} M_{,j}(\mathbf{x},g) + \beta \delta_{jn} Mi(\mathbf{x},g)\}, \tag{A1d}$$

$$I^s_{nji} = \frac{\lambda+\mu}{\lambda+2\mu}\psi_{,ijn} - \frac{\lambda}{\lambda+2\mu}\delta_{ij}\phi_{,n} - \delta_{in}\phi_{,j} - \delta_{jn}\phi_{,i}. \tag{A1e}$$

Here, $B = \kappa/[\mu(2\mu+\kappa)]$, $g^2 = (2\mu+\kappa)\gamma/(4\mu\kappa)$, and $h^2 = (\alpha+\beta+\gamma)/(2\kappa)$.

APPENDIX B: EDD DERIVATIVES FOR SPHERICAL INHOMOGENEITIES

The derivatives of $M(x_i,k)$ can be written as (Ref. 19):

$$M_{,i}(\mathbf{x},k)=x_i\frac{\Phi(k)}{ikr}j_1(ir/k), \tag{B1a}$$

$$M_{,ij}(\mathbf{x},k)=\delta_{ij}\frac{\Phi(k)}{ikr}j_1(ir/k)-x_ix_j\frac{\Phi(k)}{k^2r^2}j_2(ir/k), \tag{B1b}$$

$$M_{,ijm}(\mathbf{x},k)=-(x_i,\delta_{jm}+x_j\delta_{im}+x_m\delta_{ij})\frac{\Phi(k)}{k^2r^2}j_2(ir/k) - x_ix_jx_m\frac{\Phi(k)}{ik^3r^3}j_3(ir/k), \tag{B1c}$$

$$M_{,ijmn}(\mathbf{x},k)=-(\delta_{ij}\delta_{mn}+\delta_{im}\delta_{jn}+\delta_{in}\delta_{jm})\frac{\Phi(k)}{k^2r^2}j_2(ir/k) -(x_ix_j\delta_{mn}+x_ix_m\delta_{jn}+x_ix_n\delta_{jm}+x_jx_m\delta_{in} +x_jx_n\delta_{im}+x_nx_m\delta_{ij})\frac{\Phi(k)}{ik^3r^3}j_3(ir/k) +x_ix_jx_mx_n\frac{\Phi(k)}{k^4r^4}j_4(ir/k). \tag{B1d}$$

Here j_v is the spherical Bessel function of order v. It can be written in terms of the Bessel function of first kind (of half-integers), $J_{v+1/2}$, i.e.,

$$j_\nu(z)=\frac{1}{\sqrt{z}}\sqrt{\tfrac{\pi}{2}}J_{\nu+1/2}(z). \tag{B2}$$

APPENDIX C: *P* INTEGRALS USED IN EQ. (12) (FOR SPHERICAL INHOMOGENEITY)

Using Eq. (11) and (14), all of the averages can be expressed in terms of the following integrals:

$$P_1(k)=\int_\Omega\int\int\frac{\sinh(r/k)}{r}dV, \tag{C1a}$$

$$P_2(k)=\int_\Omega\int\int\frac{j_{1^{(ir/k)}}}{r}dV, \tag{C1b}$$

$$P_{3ij}(k)=\int_\Omega\int\int\frac{x_ix_jj_{1^{(ir/k)}}}{r}dV, \tag{C1c}$$

$$P_4(k)=\int_\Omega\int\int\frac{j_{2^{(ir/k)}}}{r^2}dV, \tag{C1d}$$

$$P_{5ij}(k)=\int_\Omega\int\int\frac{x_ix_jj_{3^{(ir/k)}}}{r^3}dV, \tag{C1e}$$

$$P_{6ijkl}(k)=\int_\Omega\int\int\frac{x_ix_jx_kx_lj_{4^{(ir/k)}}}{r^4}dV. \tag{C1f}$$

More details of the evaluation of average Eshelby's tensors are omitted for the sake of brevity, but it is noted that integrals involving odd combinations of position vector average to zero (i.e., x_i, or $x_ix_jx_k$, etc.) When the integrand contains even combination of position vector (i.e., x_ix_j), all combinations in which the indices are not identical also average to zero. As an example, integrals of $x_ix_jx_k$ multiplied by any combination of r or the Bessel function is zero (odd combination), while x_ix_j is zero whenever $i\neq j$ (even combination). This greatly simplifies the derivation.

The integration has been performed, and the results are

$$P_1(k)=4\pi[ak\cosh(a/k)-k^2\sinh(a/k)], \tag{C2a}$$

$$P_2(k)=4\pi ik^2[\sinh(\alpha/k)-\mathrm{Shi}(a/k)], \tag{C2b}$$

$$P_{3ij}(k)=\frac{4\pi k^2}{3}[-a\cosh(a/k)+4k\sinh(a/k) -3k\mathrm{Shi}(a/k)] \quad \text{if } i=j=0 \quad \text{if } i\neq j, \tag{C2c}$$

$$P_4(k)=\frac{2\pi}{a^2}[k\{3k(-a\cosh(a/k)+k\sinh(a/k)) +a^2\,\mathrm{shi}(a/k)\}], \tag{C2d}$$

$$P_{5ij}(k)=\frac{-2\pi}{3a^2}[ik^2(-15ak\cosh(a/k) +(2a^2+15k^2)\sinh(a/k)+3a^2\,\mathrm{shi}(a/k))] \quad \text{if } i=j=0 \quad \text{if } i\neq j, \tag{C2e}$$

$$P_{6ijkl}(k)=\frac{2\pi}{5a^2}[k^2(a(2a^2+105k^2)\cosh(a/k)-k(22a^2 +105k^2)\sinh(a/k)-15a^2k\sinh(a/k))] \quad \text{if } i=j=0 \quad \text{if } i\neq j. \tag{C2f}$$

Here Shi indicates the sinh integral.

APPENDIX D: DERIVATIVES OF EDD, HARMONIC, AND BIHARMONIC FUNCTIONS FOR CYLINDRICAL INHOMOGENEITIES

The average of derivatives of $M(x_i,k)$ can be written as (see Ref. 20)

$$\langle M(\mathbf{x},k)\rangle=k^2-k^2J_1\left(\frac{a}{k}\right)K_1\left(\frac{a}{k}\right), \tag{D1a}$$

$$M_{,3}(\mathbf{x},k)=0, \tag{D1b}$$

$$\langle M_{,i}(\mathbf{x},k)\rangle=0, \tag{D1c}$$

$$\langle M_{,ij}(\mathbf{x},k)\rangle=-J_1\left(\frac{a}{k}\right)K_1\left(\frac{a}{k}\right)\delta_{ij}, \tag{D1d}$$

$$\langle M_{,ijk}(\mathbf{x},k)\rangle=0, \tag{D1e}$$

$$\langle M_{,ijkl}(\mathbf{x},k)\rangle=-\frac{(\delta_{ij}\delta_{mn}+\delta_{im}\delta_{jn}+\delta_{in}\delta_{jm})}{4k^2}J_1\left(\frac{a}{k}\right)K_1\left(\frac{a}{k}\right). \tag{D1f}$$

J and K are the modified Bessel functions of the first and second kinds, respectively. The average of derivatives of ϕ and ψ can be written as[15]

$$\langle \phi_{,ij}\rangle=-\delta_{ij}T_I, \tag{D2a}$$

$$\langle \psi_{,ijkl}\rangle=-\delta_{ij}\delta_{kl}[T_K-a_I^2T_{IK}]-(\delta_{ik}\delta_{jl}+\delta_{jk}\delta_{il})[T_J-a_I^2T_{ij}],$$

$$T_I=T_2=2\pi, \quad T_3=0, \tag{D2b}$$

$$T_{12}=\frac{\pi}{a^2}, \tag{D3a}$$

$$3T_{11}=\frac{4\pi}{a^2}-T_{12}, T_{22}=T_{11}, \tag{D3b}$$

$$T_{13}=T_{23}=T_{33}=0, \tag{D3c}$$

$$a_3^2T_{23}=a_3^2T_{13}=T_1, a_3^2T_{33}=0. \tag{D3d}$$

Note that capital subscripts are used to indicate that there is to be no summation over repeated indices. $a_1=a_2=a$ is the radius of the circular cylinder. a_3 is of course unbounded, but [as is apparent from Eq. (D3d)] the limit, when its square is multiplied by the "T" parameters, is bounded.

*Email address: sharma@crd.ge.com

[1] A. C. Eringen, *Microcontinuum Field Theories I: Foundations and Solids*, (Springer-Verlag, New York, 1999).
[2] R. Lakes, in *Continuum Models for Materials with Microstructure*, edited by H. B. Mühlhaus (Wiley, New York, 1995).
[3] A. C. Eringen, J. Math. Mech. **15**, 909 (1966).
[4] A. C. Eringen, in *Theory of Micropolar Elasticity*, Fracture, Vol II, edited by H. Liebowitz (Academic, New York, 1968).
[5] A. C. Eringen and C. B. Kafadar, *Polar Field Theories*, Continuum Physics, Vol. IV (Academic, New York, 1976).
[6] W. Nowaki, *Theory of Micropolar Elasticity* (Springer-Verlag, Wien, 1970).
[7] W. Nowaki, *Theory of Asymmetric Elasticity* (Polish-Scientific, Warszawa, 1986).
[8] M. Ciarletta, and D. Iesan, *Non-classical Elastic Solids* (Longman, London, 1993).
[9] H. B. Mühlhaus, *Continuum Models for Materials with Microstructure* (Wiley, New York, 1995).
[10] W. B. Anderson and R. S. Lakes, J. Mater. Sci. **29**, 6413 (1994).
[11] Frederic Bouyge, Iwona Jasiuk, and Martin Ostoja-Starzewski, 1999 *Bioengineering Conference, Big Sky, MT, USA, American Society of Mechanical Engineers, Bioengineering Division (Publication) BED*, V 42 1999.
[12] J. F. C. Yang and R. S. Lakes, J. Biomech. **15**, 91 (1982).
[13] I. A. Ovid'ko, Science **295**, 2386 (2002).
[14] M. Murayama, J. M. Howe, H. Hidaka, and S. Takaki, Science **295**, 2433 (2002).
[15] T. Mura, *Micromechanics of Defects in Solids* (Martinus Nijhoff, Hague, Netherlands, 1987).
[16] T. Mura, H. M. Shodja, and Y. Hirose, Appl. Mech. Rev. **49**, S118 (1996).
[17] T. Mura, Mater. Sci. Eng., A **285**, 224 (2000).
[18] S. Nemat-Nasser and M. Hori, *Micromechanics: Overall Properties of Heterogeneous Solids* (Elsevier, Amsterdam, 1999).
[19] Z. Q. Cheng and L. H. He, Int. J. Eng. Sci. **33**, 389 (1995).
[20] Z. Q. Cheng and L. H. He, Int. J. Eng. Sci. **35**, 659 (1997).
[21] X. Yuan and Y. Tomita, Key Eng. Mater. **117–180**, 53 (2000).
[22] X. Yuan and Y. Tomita, Mech. Res. Commun. **28**, 265 (2001).
[23] S. Forest, *Multiscale Modeling of Materials-2000, Boston, MA* edited by L. P. Kubin, J. L. Bassani, K. Cho, H. Gao, R. L. B. Selinger, MRS Symposia Proceedings No. 653 (Materials Research Society, Pitsburgh, 2001), p. 78.2.1.
[24] S. Forest, F. Barbe, and G. Cailletaud, Int. J. Solids Struct. **37**, 7105 (2000).
[25] J. D. Eshelby, Proc. R. Soc. London, Ser. A **241**, 376 (1957).
[26] J. D. Eshelby, Proc. R. Soc. London, Ser. A **252**, 561 (1959).
[27] Y. Benveniste, Mech. Mater. **6**, 147 (1987).
[28] T. Mori and K. Tanaka, Acta Metall. **21**, 571 (1973).
[29] R. Furuhashi, J. H. Huang, and T. Mura, J. Appl. Mech. **59**, 783 (1992).
[30] C. Q. Ru and P. Schiavone, Proc. R. Soc. London, Ser. A **453**, 2551 (1997).
[31] Z. Zhong and S. A. Meguid, J. Appl. Mech. **63**, 877 (1996).
[32] P. Sharma and A. Dasgupta, General Electric Corp. R & D, Class A Internal Report No. 2001CRD110, 2001.
[33] H. Nozaki and M. Taya, J. Appl. Mech. **68**, 441 (2001).
[34] G. Rodin, J. Appl. Mech. **64**, 278 (1998).
[35] H. Nozaki and M. Taya, J. Appl. Mech. **64**, 495 (1997).